On the Boundary Integral Equation Representation for Solar Magnetic Field Problems

Yihua YAN

National Astronomical Observatories

Chinese Academy of Sciences

Beijing 100012, China

Solar Radio Spectropolariometers at Huairou/Beijing

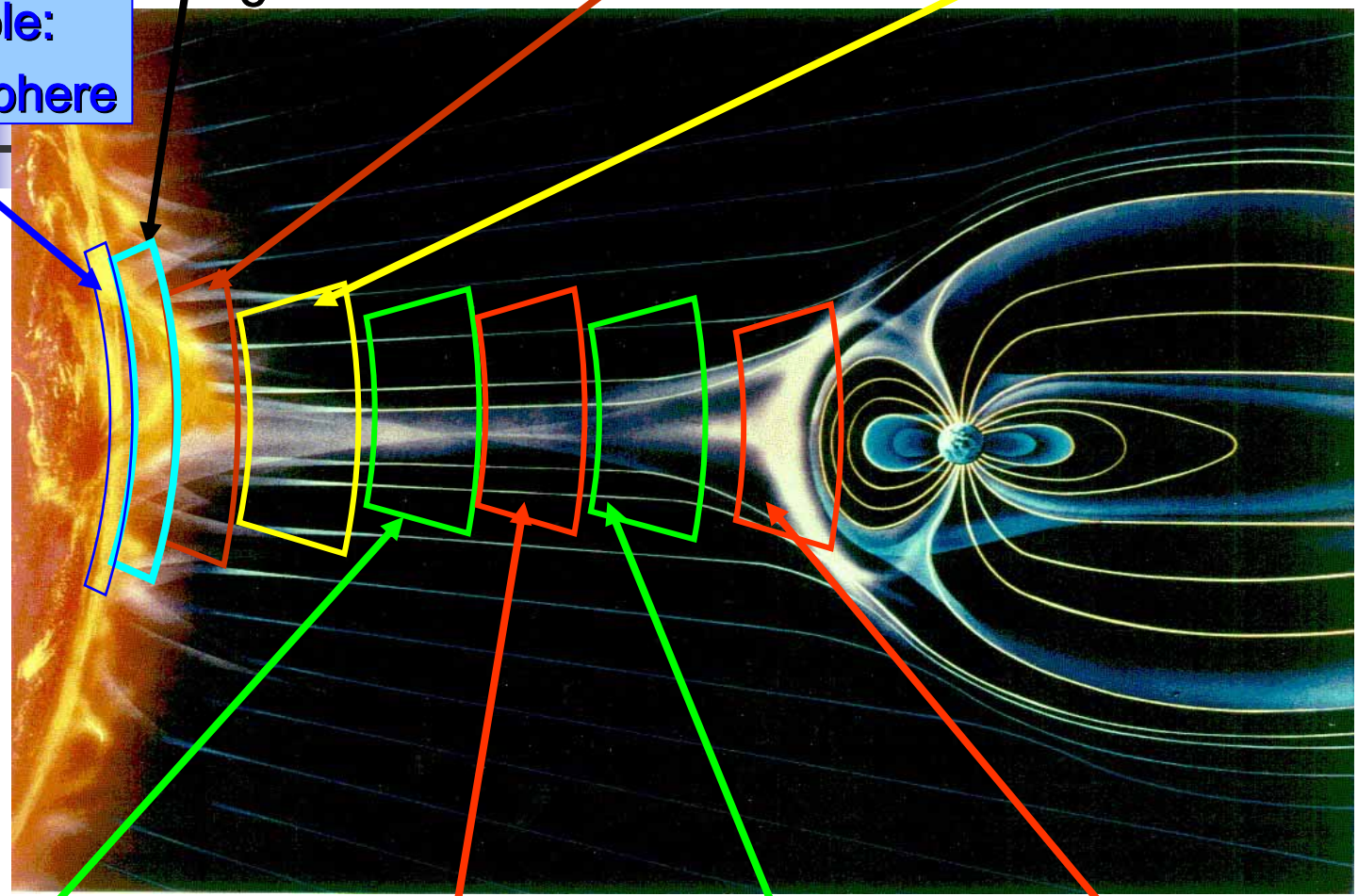
mm-waves
Chromospher
e
cm-waves: up
chrom. & corona
bottom
dm-waves:
low corona
Visible:
Photosphere
metric waves:
corona
Decametric
(30MHz):→2R⊙
2MHz:→10R⊙
~10 KHz
→200R⊙,1A
U

Outline

I. Introduction
II. Coronal Magnetic Field Modeling
III. Results
IV. Summaries

I. Introduction

- Solar flares & coronal mass ejections (CMEs) etc. are believed due to re-organization of coronal magnetic field.
- Magnetic field plays a central role in the solar activities.
- At present reliable magnetic field measurements are still confined to a few lower levels, e.g., at the photosphere and the chromosphere.

Solar Atmosphere:

Corona
(in Extreme
Ultraviolet/EUV)

Chromosphere
(in Hα)

Chromosphere
(in Ca II K)

Photosphere
(in visible light)

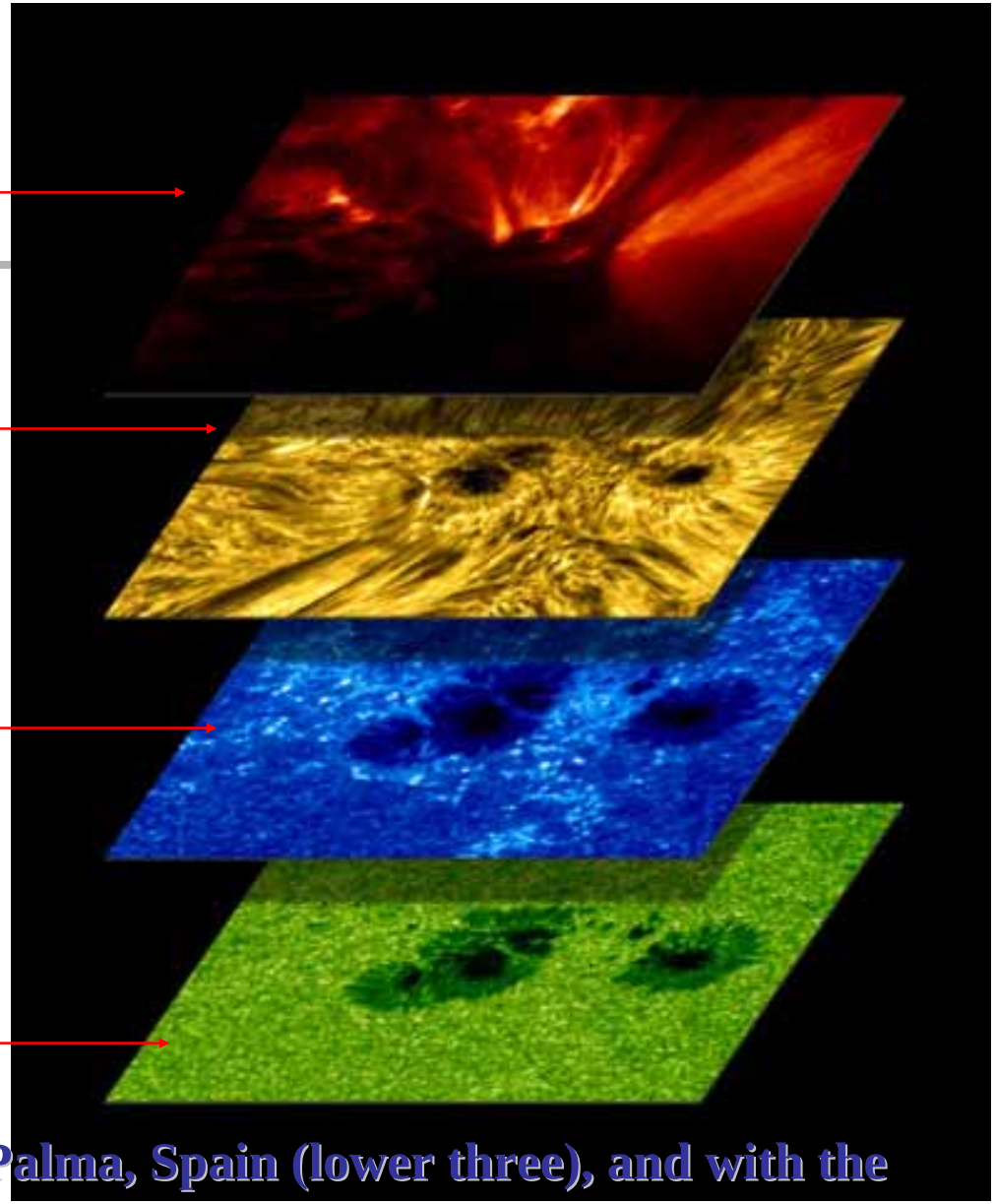

Swedish Solar Observatory on La Palma, Spain (lower three), and with the TRACE (top).

(Credit: TRACE web-site)

Approaches to study Coronal magnetic fields :

- **Infrared technique may be applied to observe the coronal magnetic field (e.g., Lin et al 2000).**
- **Radio techniques may be applied to diagnose the coronal field (e.g. VLA, or FASR) with assumptions on radiation mechanisms and propagations.**
- **Coronal Observations in EUV/UV & Soft X-Rays, etc., provide information on coronal magnetic structures.**

Explosive TRACE Loops:

Those loop or thread-like structures are believed to resemble the coronal magnetic field.

However, what we observe are plasmas, not magnetic field !

⇒Extrapolation from photospheric data upwards is still a primary tool to reconstruct coronal magnetic field.

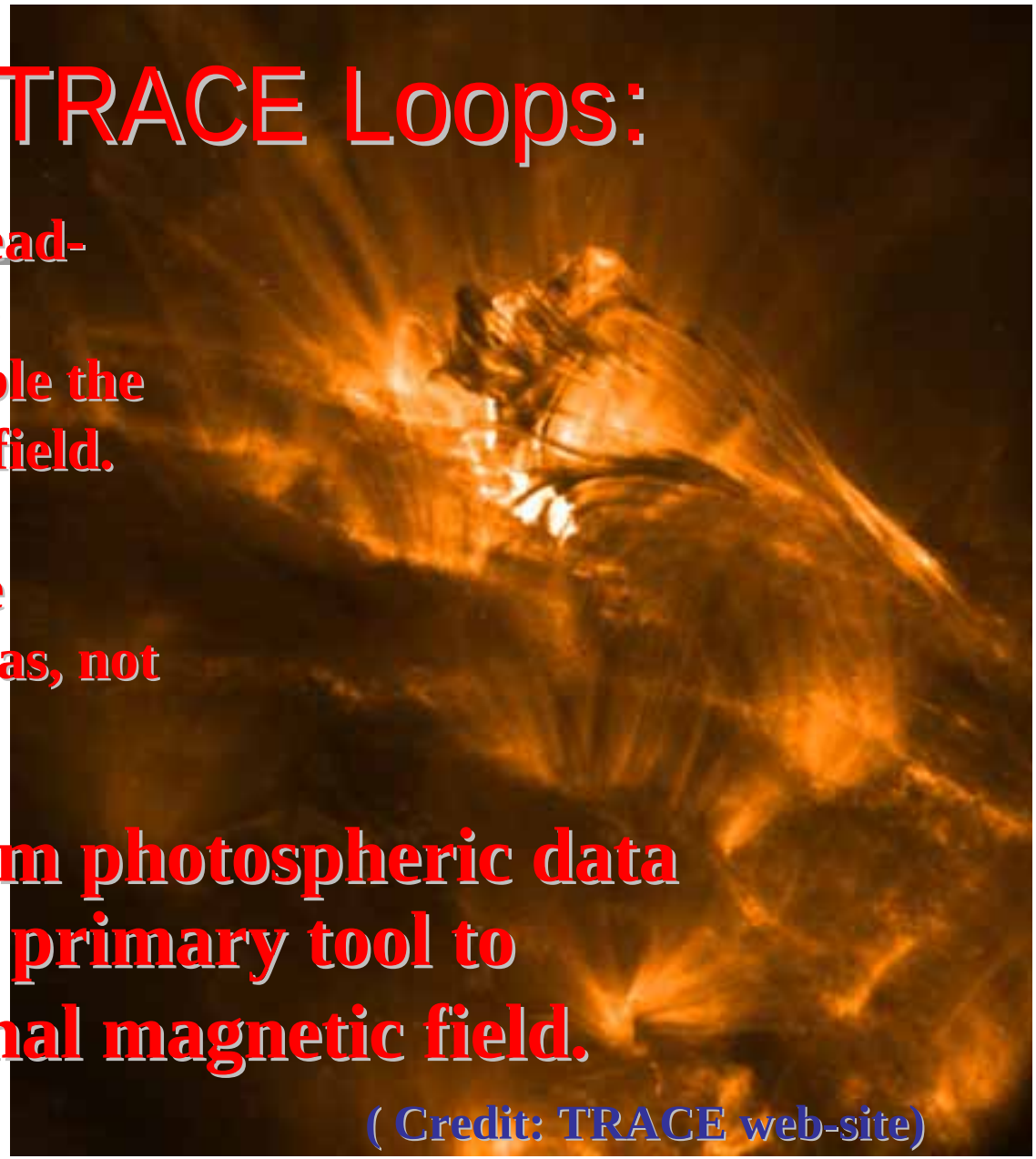

(Credit: TRACE web-site)

Coronal field configurations are important for understanding flare/CME process :

- how energy are stored, triggered, released and transported, e.g.,
  - Diagnose radio bursts;
  - Analyze HXR observations (Bob Lin);
  - Support filaments/prominences
    - 2 classes of CMES?
    - 3 part structure of CMEs?
  - Understand coronal structures;
  - Origin of fast/slow solar wind; …

II. Coronal Magnetic Field Modeling

- **Solar corona: quasi equilibrium evolution with low β plasma**
- **Models reconstructing coronal fields from observed data include potential model, linear force-free field, non-constant-α force-free field, and non-force-free field recently.**
- **PF has a** minimum energy content**. FF field can provide the** required excess ΔE**. Linear LFF models, however, have undesirable properties. In past 4 decades, reconstructing the Non-PF coronal field from boundary data** assume the magnetic field to be **FF.**

It is desired to employ non-constant-α force-free field (NLFFF)

Force-free field & divergence-free equations:

$$\mathbf{J} \times \mathbf{B} = 0, \text{ or } \nabla \times \mathbf{B} = \alpha \mathbf{B} ;$$
$$\nabla \bullet \mathbf{B} = 0$$

By `$\nabla\bullet$' both sides of the FF equation, one has:

$$\mathbf{0} = \nabla \alpha \bullet \mathbf{B}$$

It indicates that α is constant along each field line, though it is in general a function of positions. It cannot be arbitrarily specified in space but may be inferred from boundary B.

Equation (3.20) looks disarmingly simple, but very little has been done so far in understanding the nature of its solutions in general. **(Priest, 1994)**

On NLFFF modeling

- **Many efforts available for NLFFF, e.g.,**
  - **Grad-Rubin: Sakurai 1981, Amari et al. 1999**
  - **Direct-FFF Eq.: Wu et al. 1990**
  - **MHD evolution: Mikic et al 1995; Roumeliotis 1996, Valori et al. 2005**
  - **BIE: Yan & Sakurai 1997,2000**
  - **Pseudo evolution: Wheatland et al. 2000, Wiegelmann 2004**
- **BIE representation of the NLFFF (Yan & Sakurai 2000) can take into account:**
  1. **finite energy content in open space**
  2. **implementing boundary data B directly**

NLFFF (Yan & Sakurai 2000)

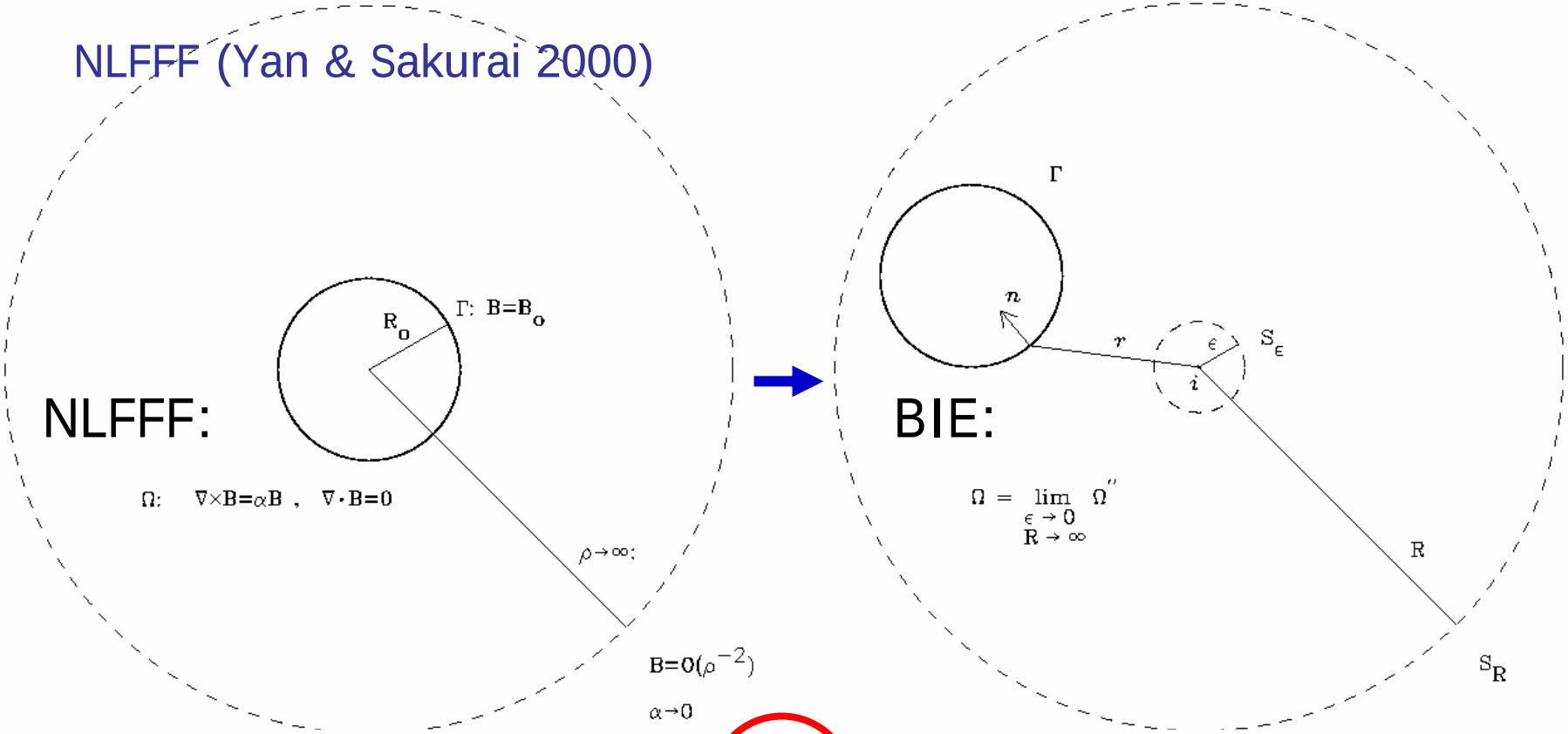

$$\mathbf{c}_i \mathbf{B}(\mathbf{r}_i) = \int_\Gamma \left[Y(\mathbf{r}_i;\mathbf{r}) \frac{\partial \mathbf{B}}{\partial n}(\mathbf{r}) - \frac{\partial Y}{\partial n}(\mathbf{r}_i;\mathbf{r}) \mathbf{B}(\mathbf{r}) \right] d\Gamma$$

($\mathbf{c}_i = 1/2$ if i in Γ ; $\mathbf{c}_i = 1$ if i in Ω)

where $$\int_\Omega Y(\mathbf{r}_i;\mathbf{r}) [\lambda^2(\mathbf{r}_i)\mathbf{B}(\mathbf{r}) - \alpha^2(\mathbf{r})\mathbf{B}(\mathbf{r}) - \nabla\alpha(\mathbf{r}) \times \mathbf{B}(\mathbf{r})] \, d\Omega = 0$$

$$Y(\mathbf{r}_i;\mathbf{r}) = \cos(\lambda|\mathbf{r} - \mathbf{r}_i|)/(4\pi|\mathbf{r} - \mathbf{r}_i|)$$

Properties of BIE Model:

- **Vector magnetic fields-[B] are needed on the bottom boundary:**
  - **only available for ARs**
  - **not yet available globally (expecting SDO, etc.?)**
- **Normal differential of the field-[$\partial B/\partial n$] on boundary has to be solved numerically:**
  - **with dense algebraic coefficient matrix**

$\Rightarrow$

Eliminate the [$\partial B/\partial n$] term? Yes!

-but only for simple geometry

New NLFFF model (Yan & Li, 2005):

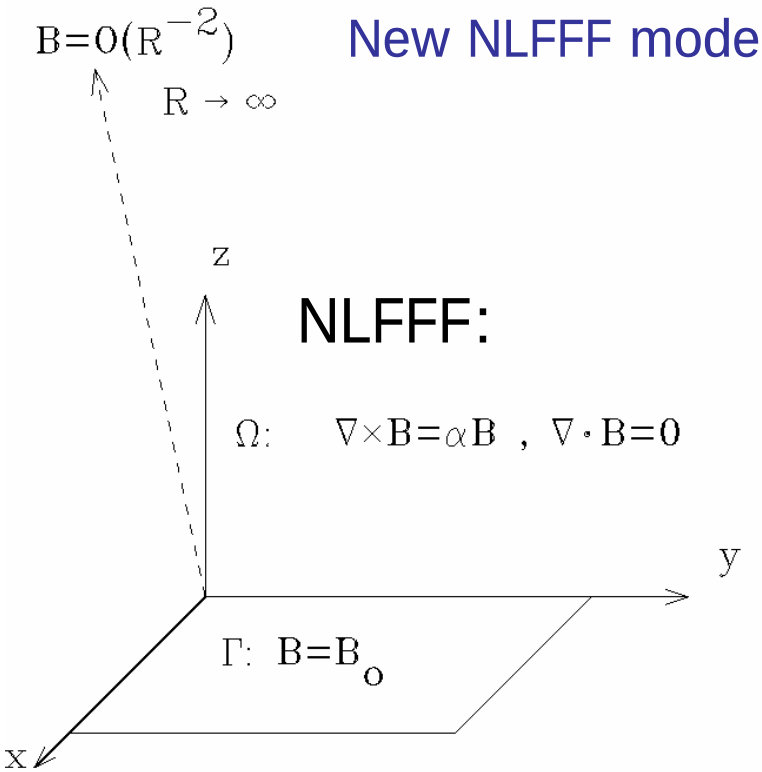

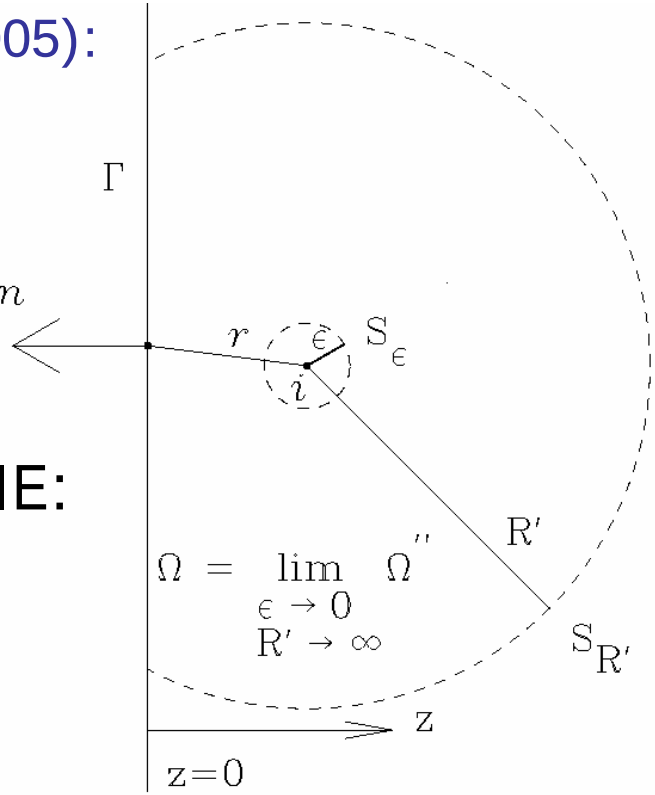

$$B_p(x_i, y_i, z_i) = \int_\Gamma \frac{z_i[\lambda r \sin(\lambda r) + \cos(\lambda r)] B_{0p}(x, y, 0)}{2\pi[(x - x_i)^2 + (y - y_i)^2 + z_i^2]^{3/2}} dxdy$$

in which λ satisfies: $\int_\Omega Y(x, y, z; x_i, y_i, z_i, \lambda)[\lambda^2 B_p - \alpha^2 B_p - (\nabla\alpha \times \mathbf{B})_p] dxdydz = 0$

where $Y = Y_1 - Y_2$, with, $Y_1 = \frac{\cos(\lambda r)}{4\pi r}$, $Y_2 = \frac{\cos(\lambda r')}{4\pi r'}$,

$r = \sqrt{(x - x_i)^2 + (y - y_i)^2 + (z - z_i)^2}$ and $r' = \sqrt{r^2 + 4z_i z}$

Such λ's in Yan&Sakurai (2000) do exist and were evaluated in Li et al. (2004, MNRAS).

Global Field Reconstruction:

- **Global field reconstruction from observed B_z data are generally modeled under current-free condition, or potential field (but may also be from MHD model, e.g., Linker et al. Wu et al.). For the source-surface method or its variants (Hoeksema, Zhao & Hoeksema, etc.):**
  - **the source-surface employed to fit the observed coronal structures**
  - **free parameter needed in order to obtain closed field region versus open field lines**
- **High resolution processing results of corona images claim to have predominantly radial open field lines (Woo et al.)**

BEM Solution of Global Potential Field:

- **The BEM solution for potential problem (Yan et al. 1993) and recently for solar coronal field (e.g., Wang et al. 2002; Yan 2005):**
  - **Observed B_z boundary data employed directly**
  - **Only asymptotic condition of no field at infinity employed**
- **The model is simply:**

$$\nabla \times \mathbf{B} = 0 \text{ and } \nabla \cdot \mathbf{B} = 0$$

$$\nabla^2 \Psi = 0 \quad \text{with } \mathbf{B} = -\nabla \Psi \quad \text{and} \quad B_n = -\frac{\partial \Psi}{\partial n}$$

III. Results

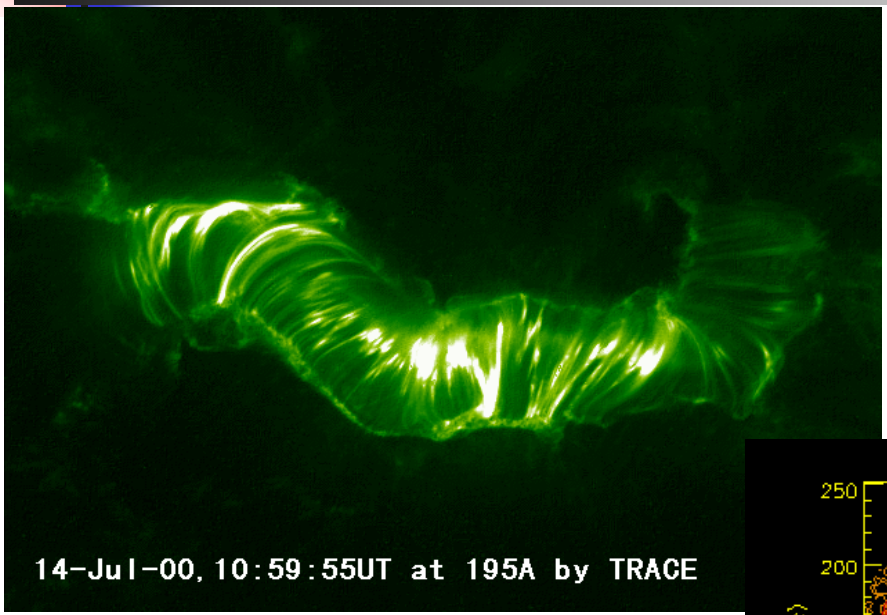

Coronal Reconstruction above ARs——
For Bastille-day event (Yan et al. 2001, *ApJ*; 2001, *Sol. Phys.*)

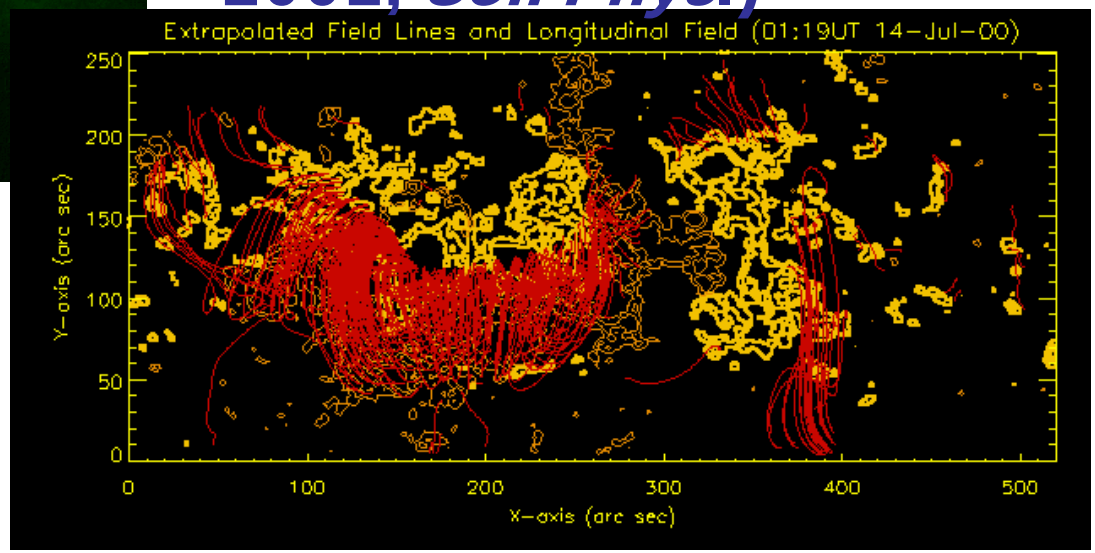

TRACE Arcades & Results

Rope dimensions

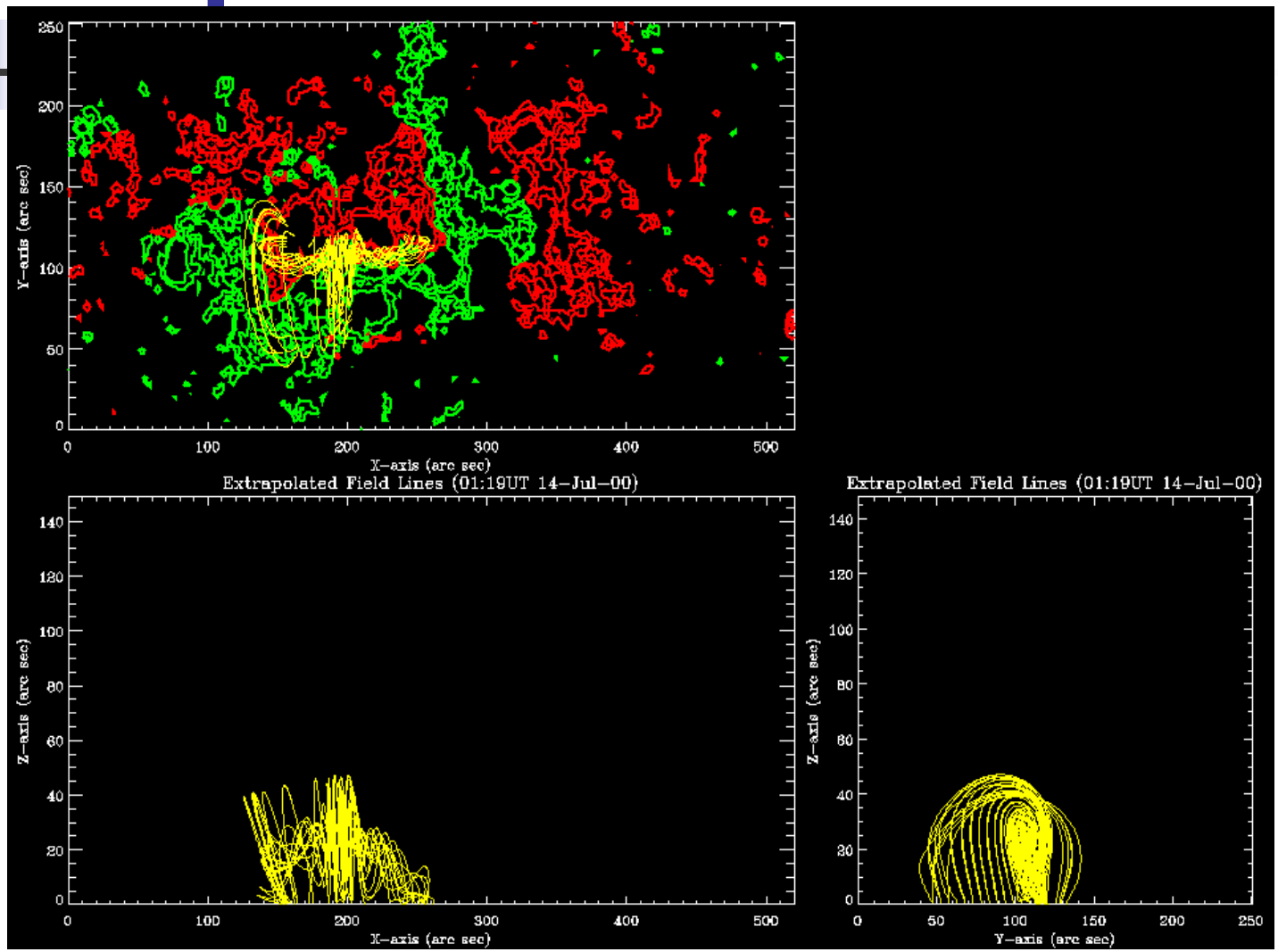

Magnetic Rope and Hα Filament

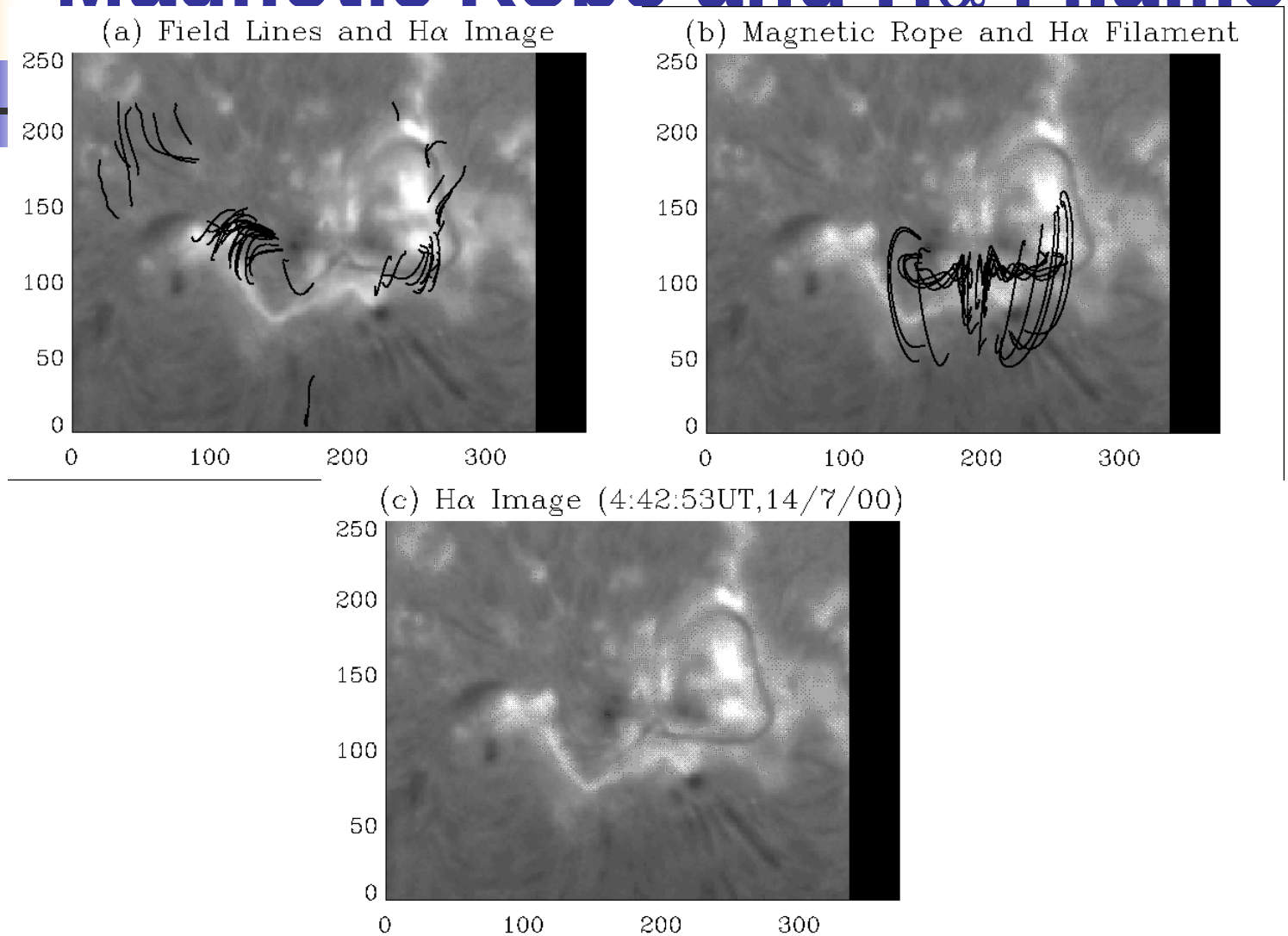

Rope and 1600A UV Bright Lane

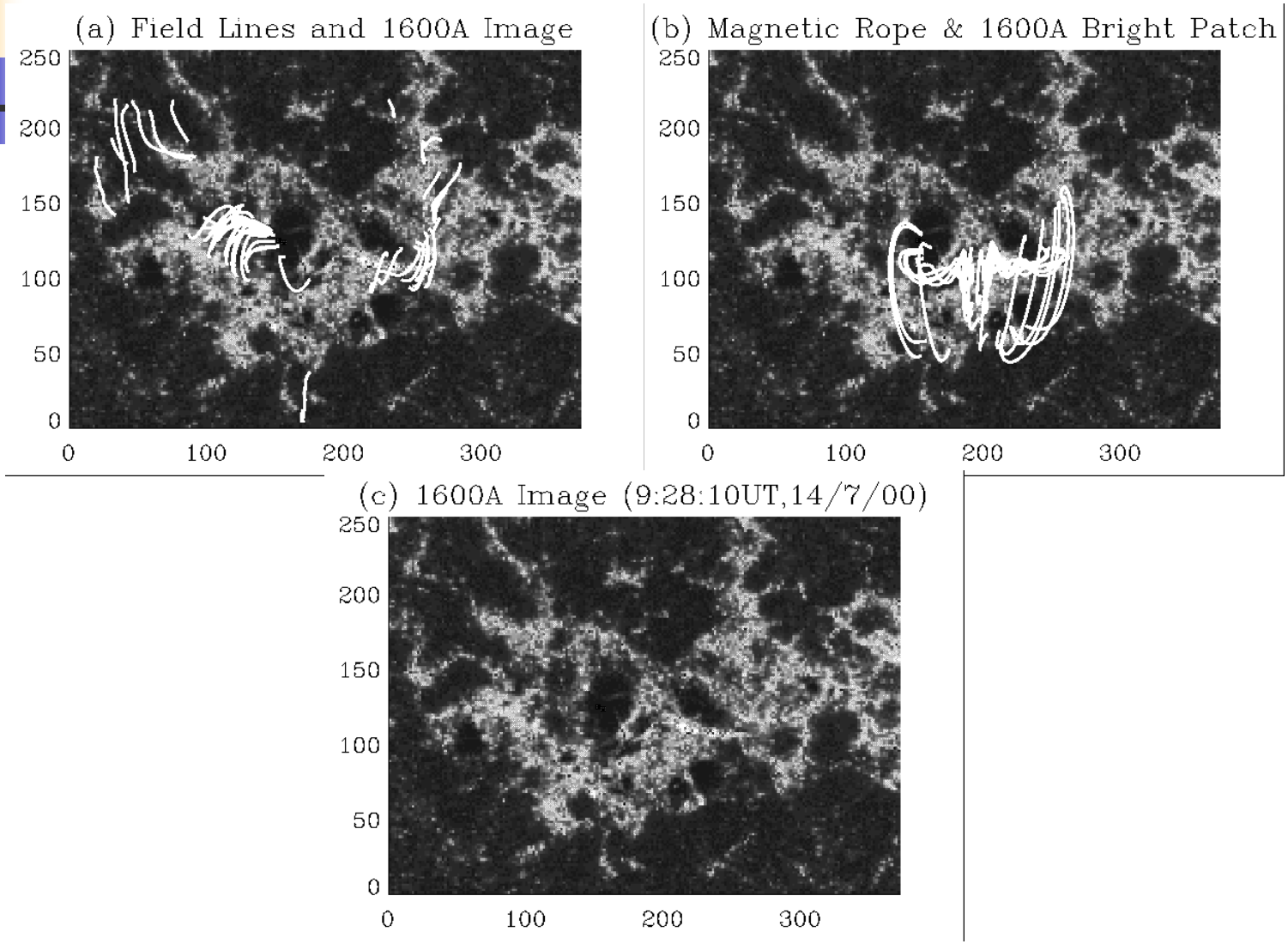

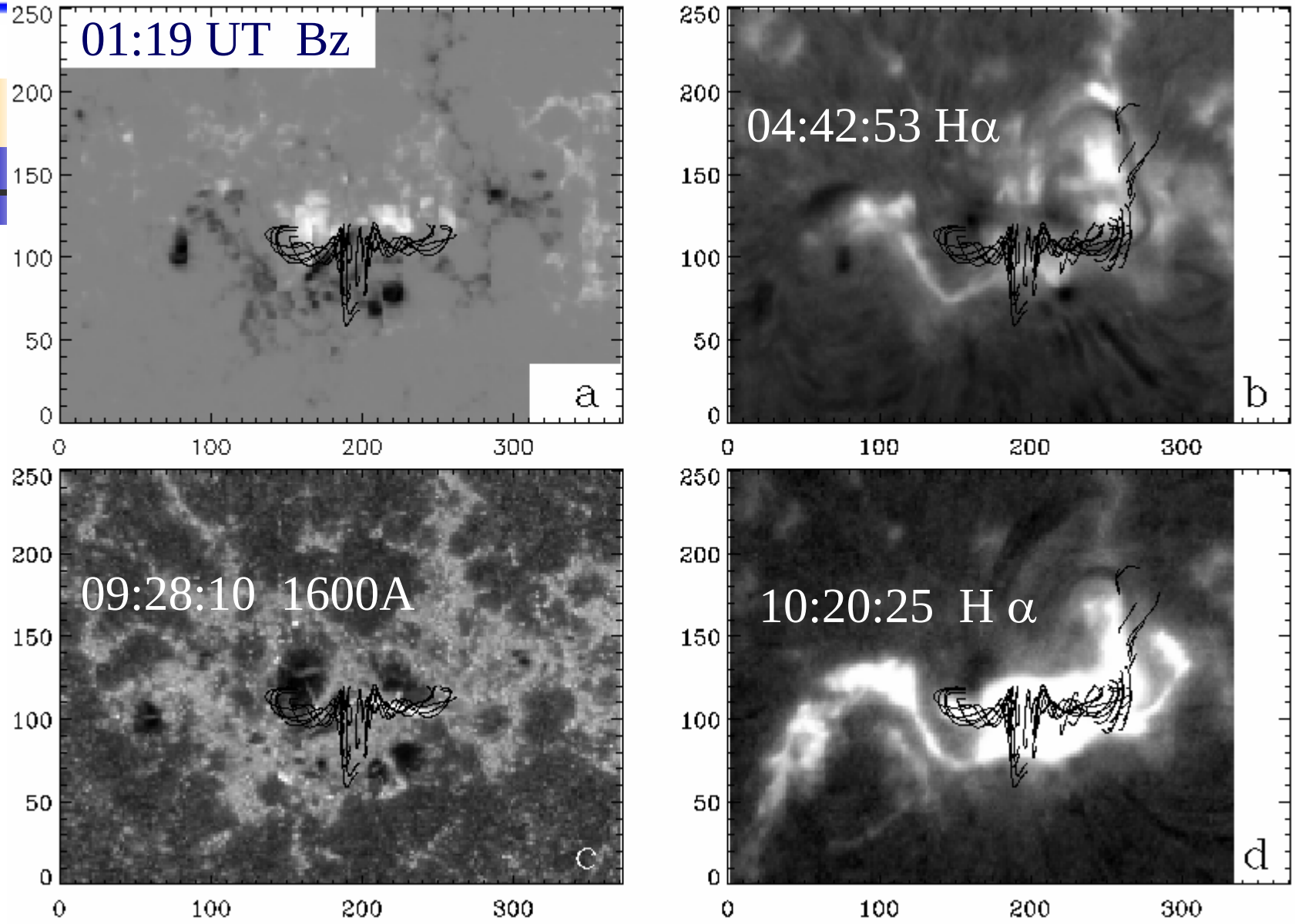
01:19 UT Bz
a
04:42:53 Hα
b
09:28:10 1600A
c
10:20:25 H α
d
0
50
100
150
200
250
300

TRACE movies

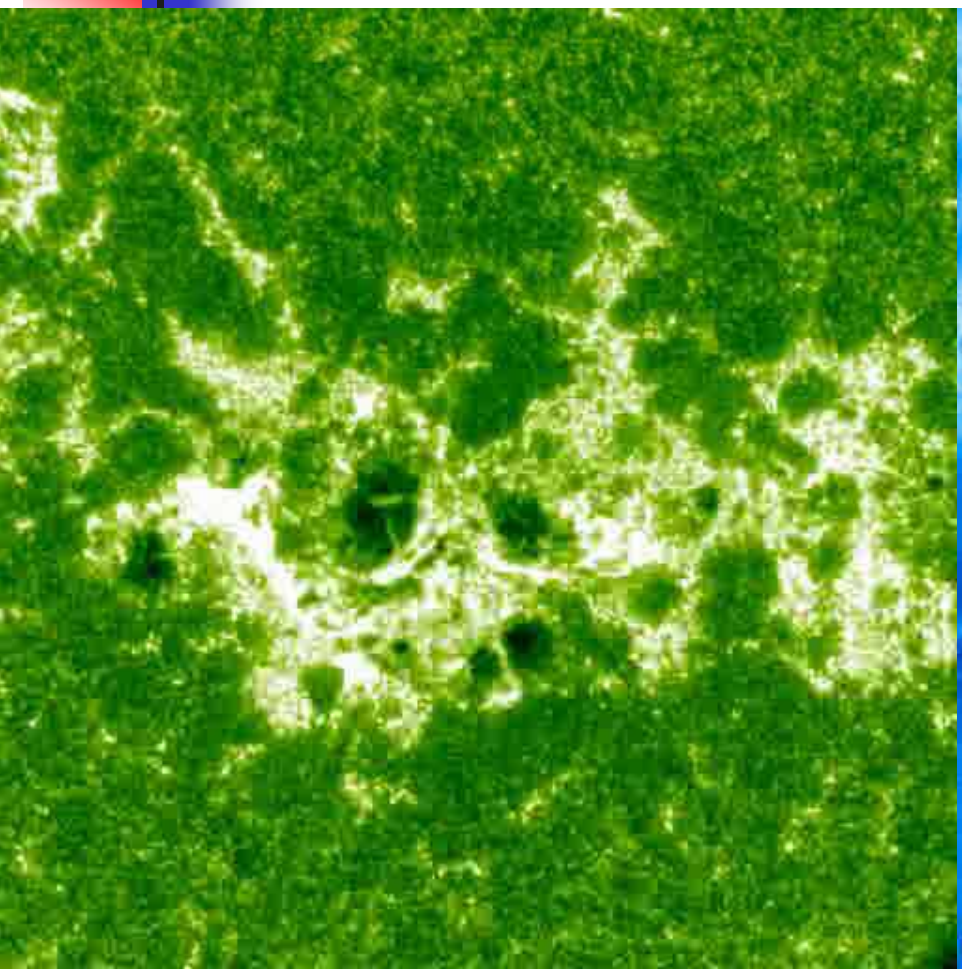

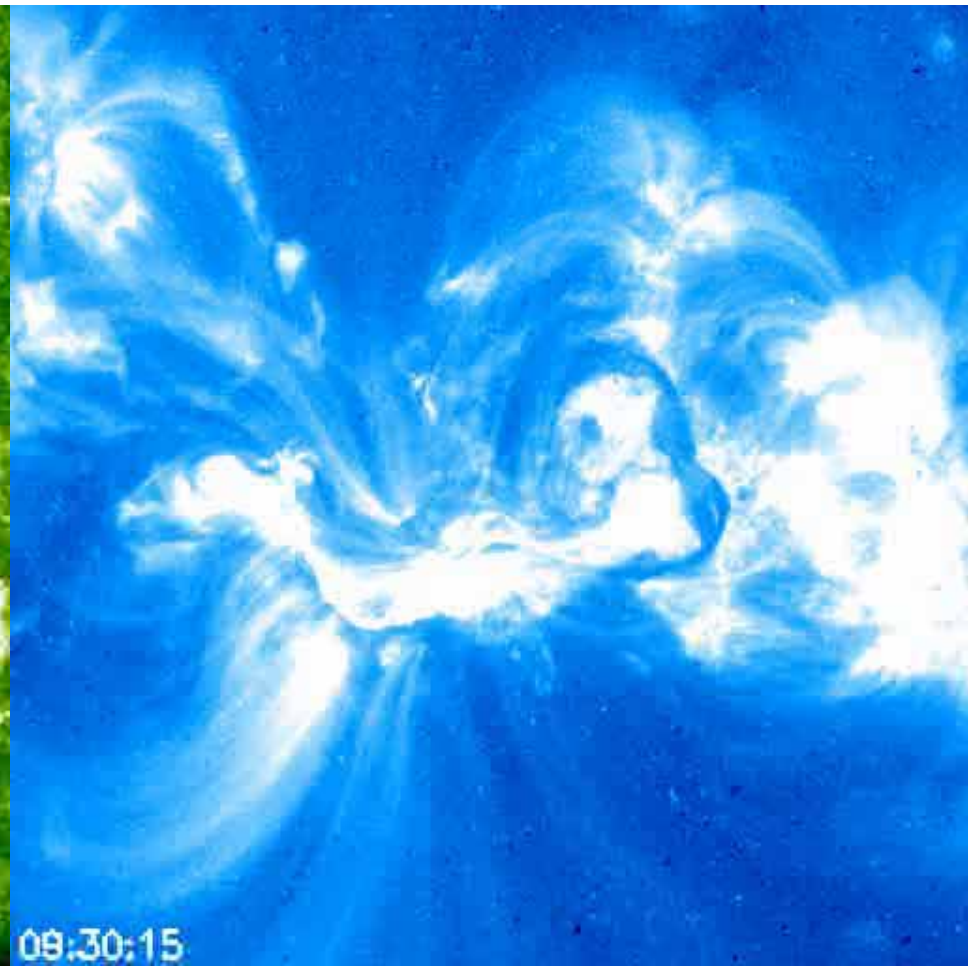

On 17-March-2002 radio burst and CME event

- The event was accompanied by a Coronal Mass Ejection (CME) observed by LASCO/SOHO.
- The RHESSI hard X-ray (HXR) emission correlated in time with the development of a type III burst group.
- A narrow white light feature interpreted as a coronal shock driven by the CME lateral expansion.

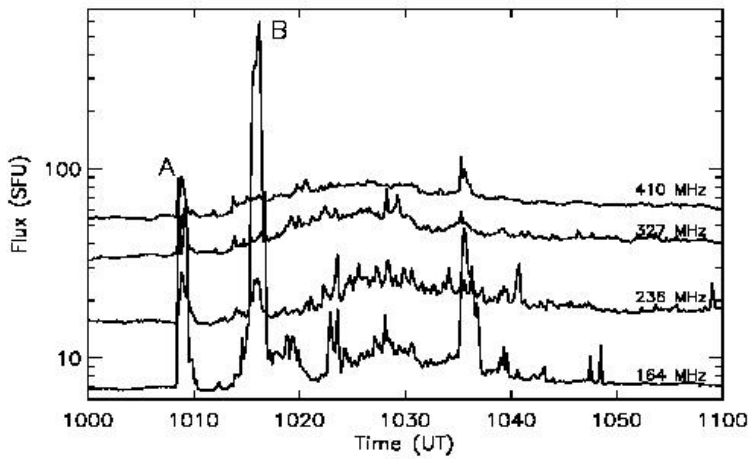

Figure 2. Global flux history of the burst on 17 March 2002.

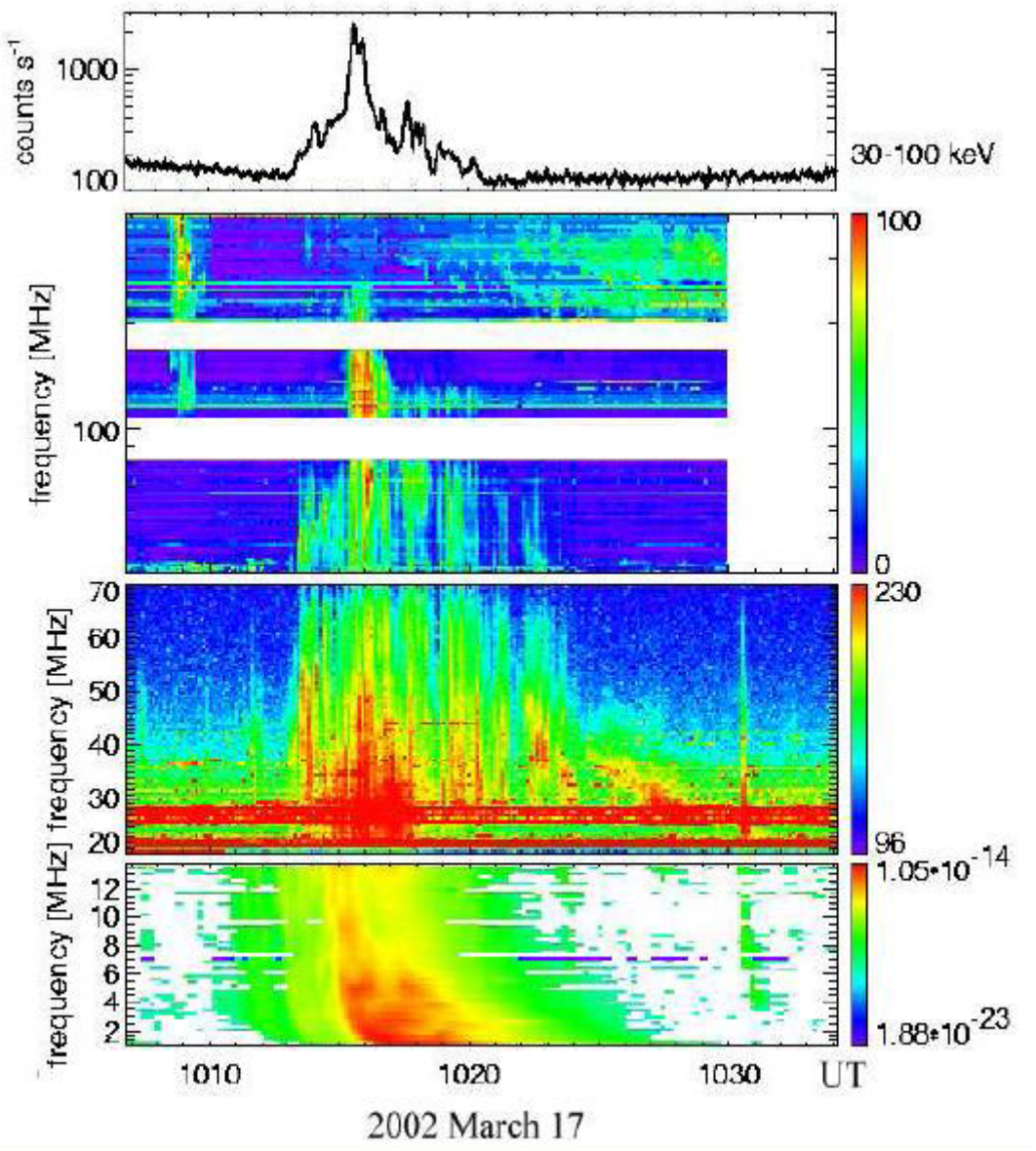

Event A

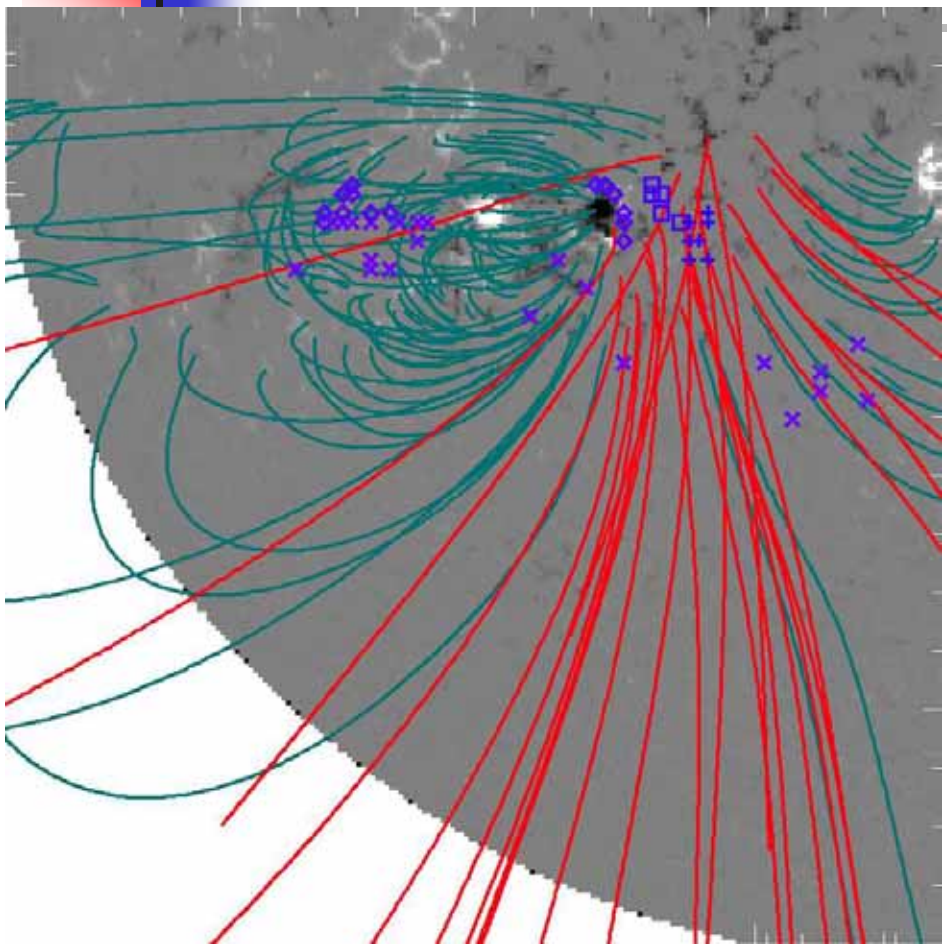

Event B

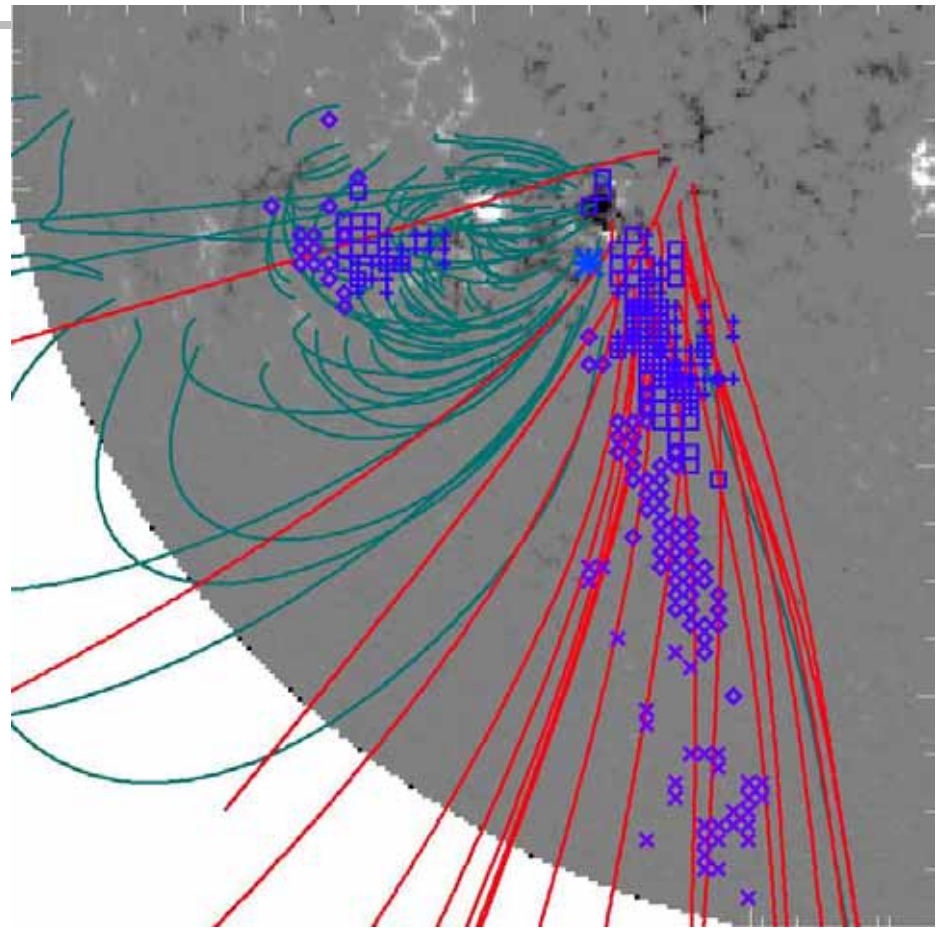

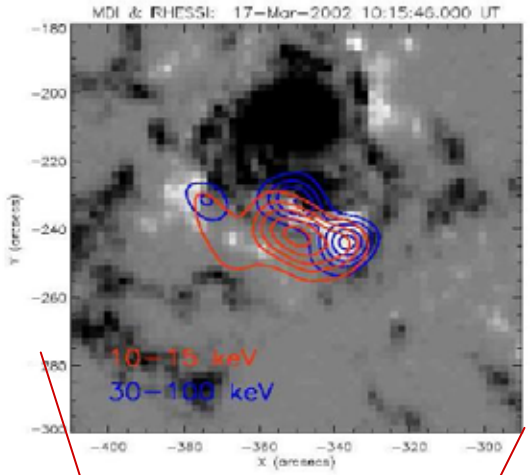

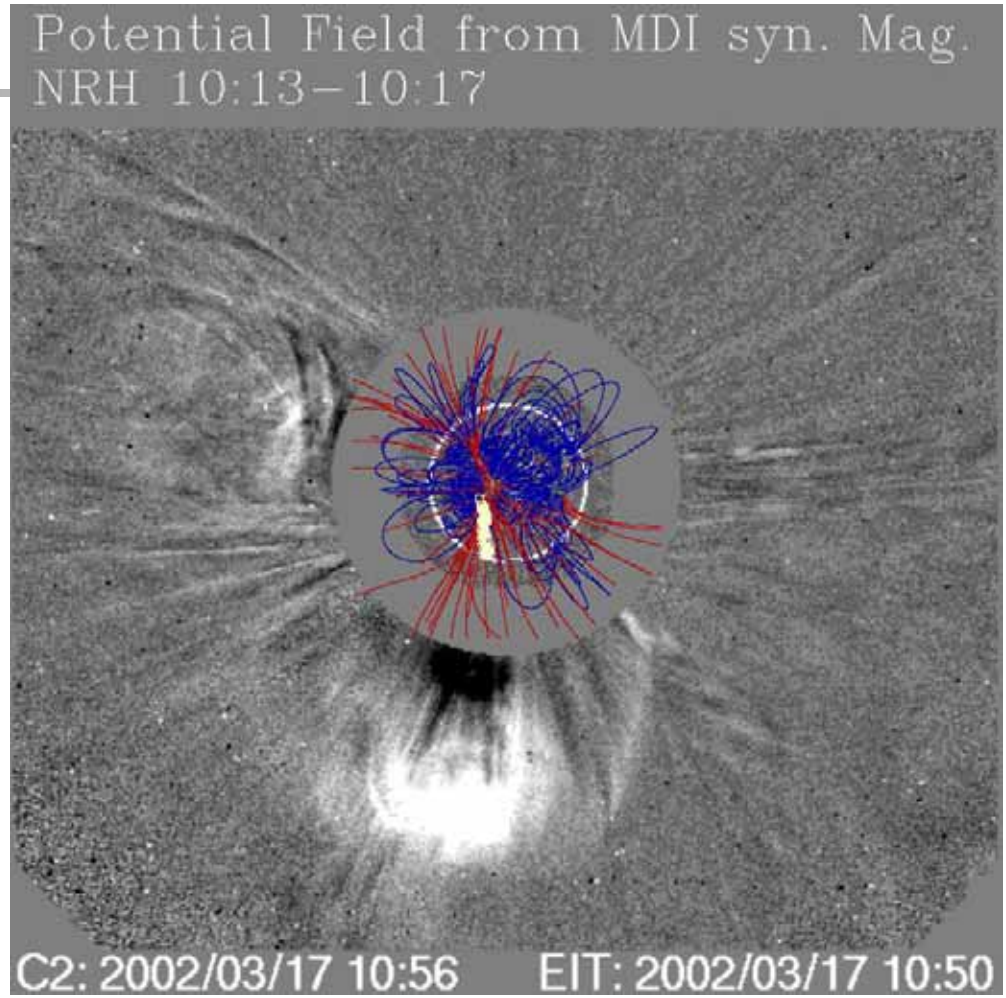

(Yan, Pick, Wang, Krucker, 2006)

5-Nov-1998 flare event

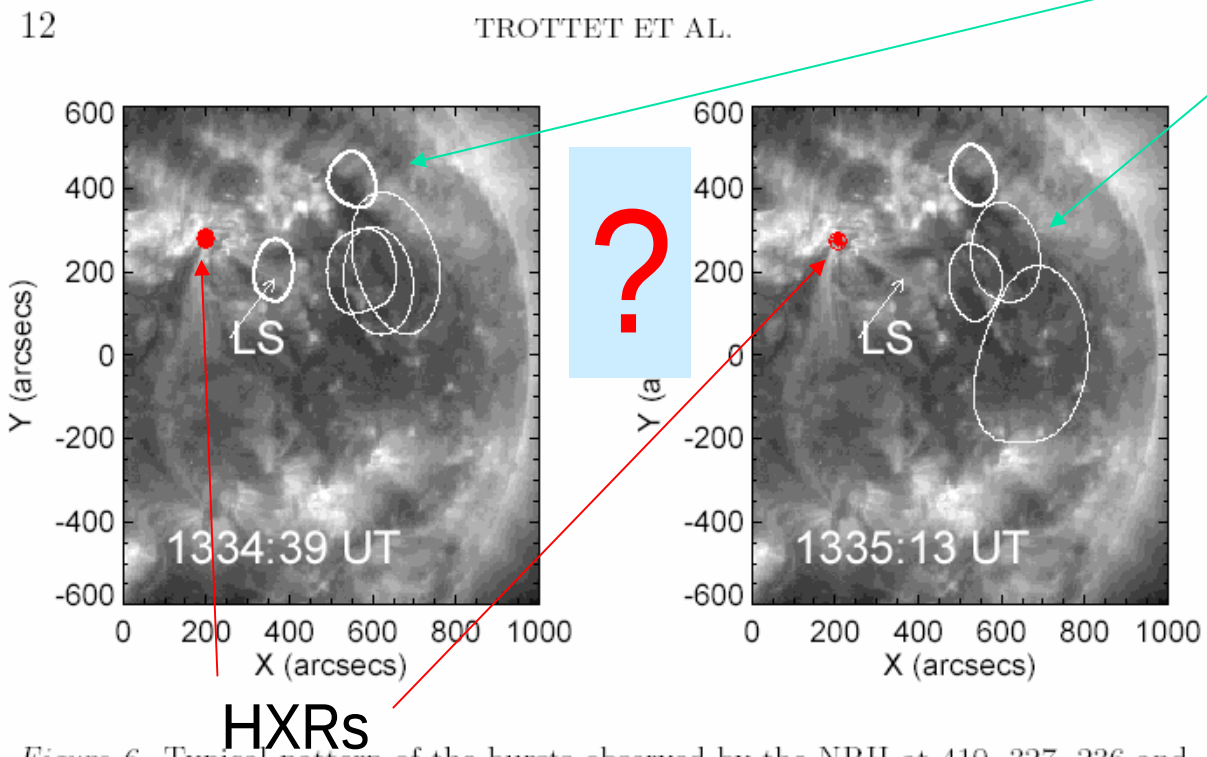

Figure 6. Typical pattern of the bursts observed by the NRH at 410, 327, 236 and 164 MHz before 1334:53 UT (left) and after 1334:53 UT (right) overlaid on the 195 Å EIT image taken at 1324:34 UT. For each frequency the contour level correspond

Radio bursts at 410, 327, 236, & 164 M with thinner lines and larger size

Trottet G., et al. (2006) Acceleration and transport during the November 5, 1998 solar flare at 1334 UT

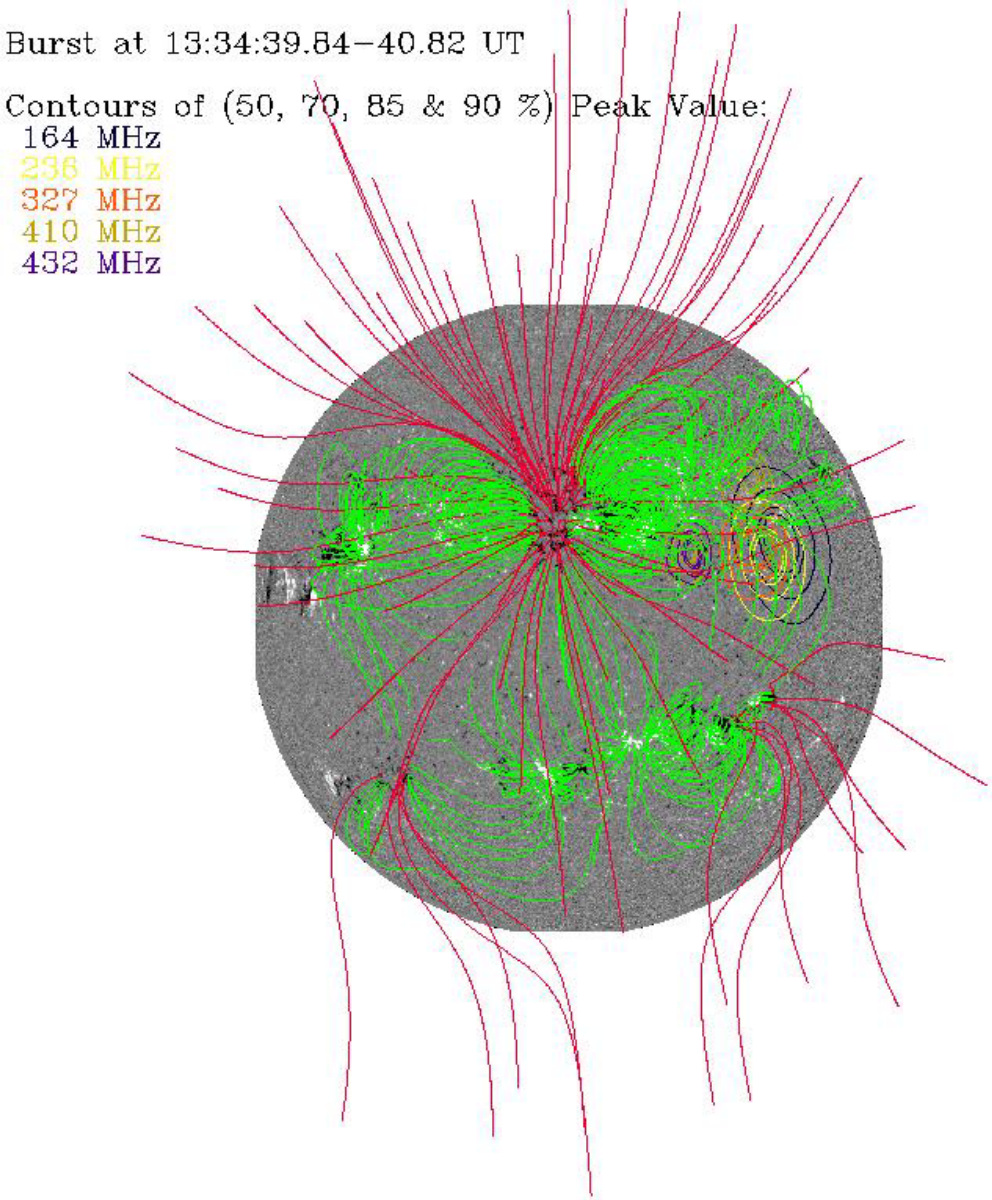
Burst at 13:34:39.84-40.82 UT
Contours of (50, 70, 85 & 90 %) Peak Value:
164 MHz
236 MHz
327 MHz
410 MHz
432 MHz

13:34 UT

Pattern I

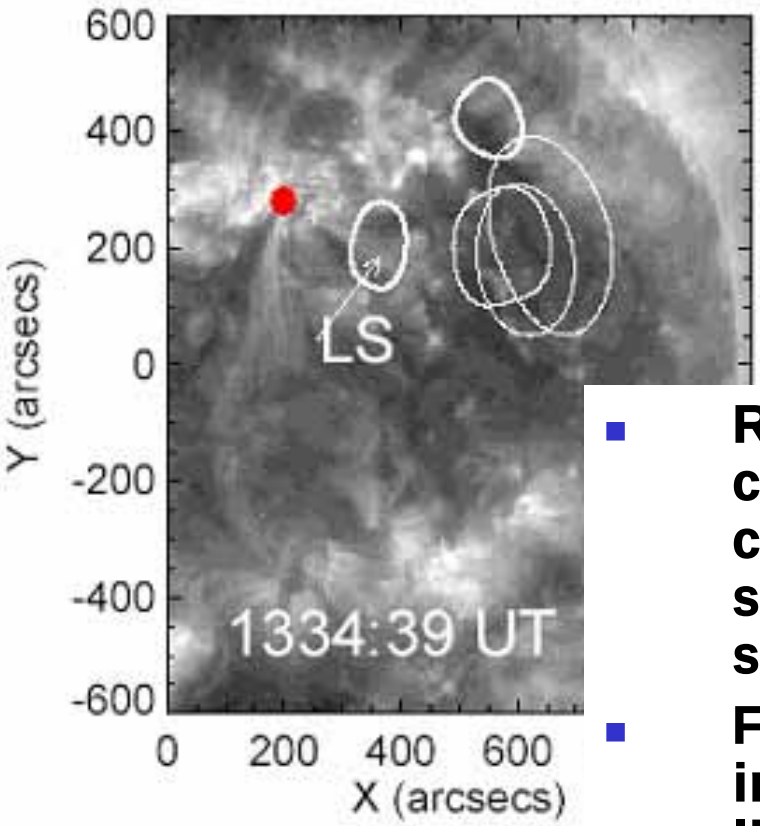

- **Radio sources at 432 and 410 MHz are connected to the HXR source region by closed field lines and they are not in the same open field lines connecting radio sources at lower frequencies.**
- **For pattern-I there might be direct injections from HXR source to the fan-like region and somehow these electrons are ejected along open lines as type III bursts.**

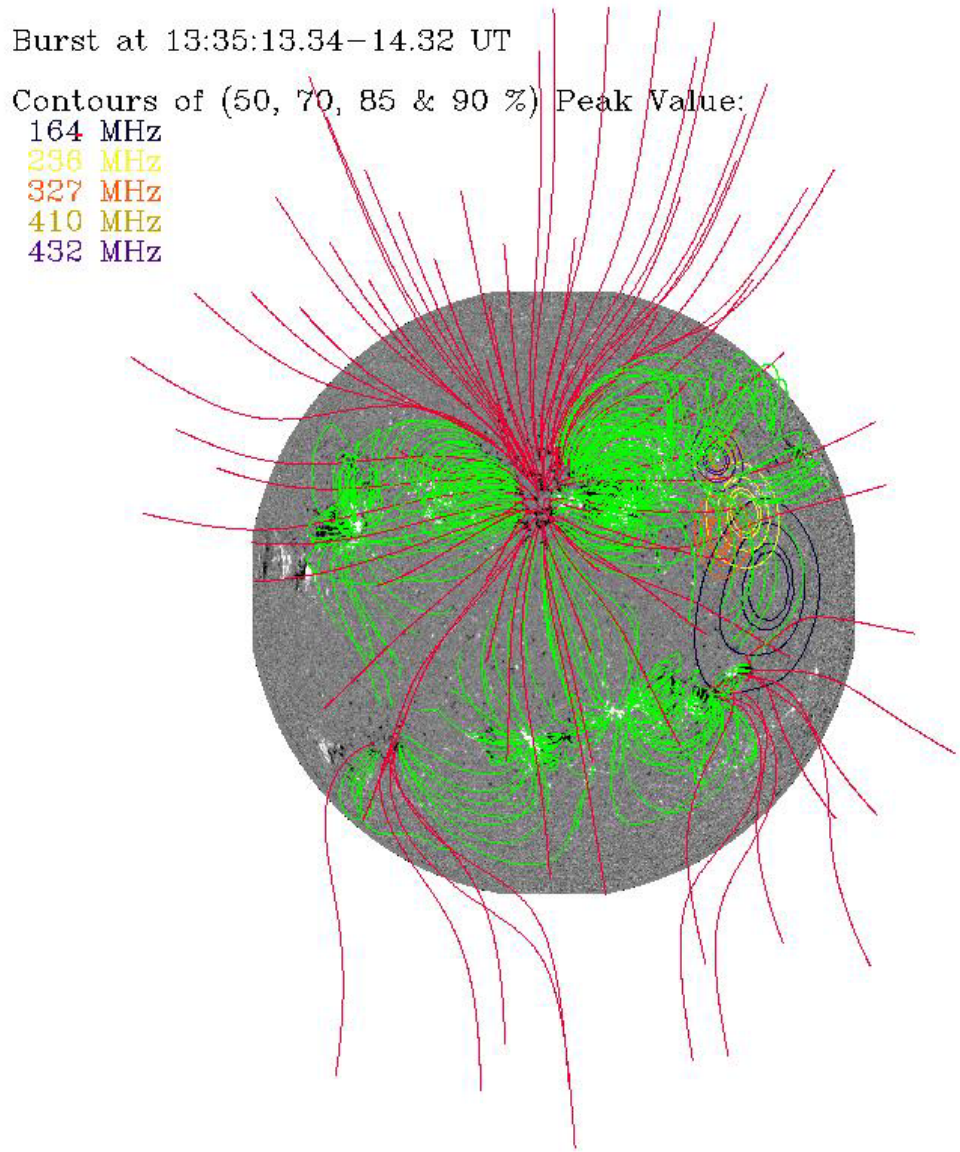
Burst at 13:35:13.34−14.32 UT
Contours of (50, 70, 85 & 90 %) Peak Value:
164 MHz
236 MHz
327 MHz
410 MHz
432 MHz

13:35 UT

Pattern II

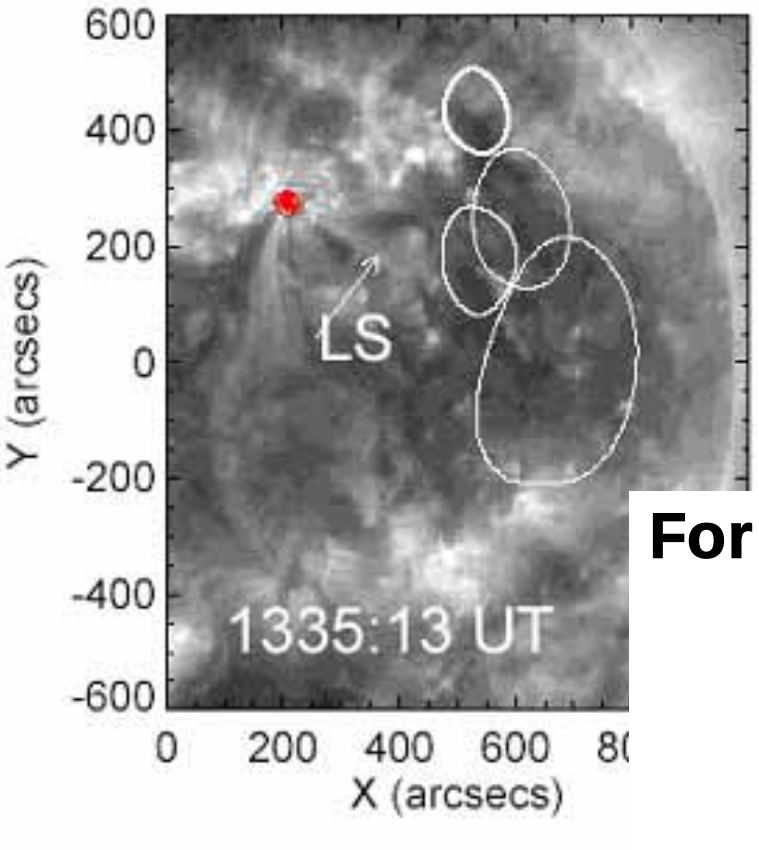

For pattern-II, we do not get field lines that connect radio sources and HXR sources directly. However, the side view of the radio sources indicates that they are in the same fan-like cusp region.

IV. Summaries

- **Reconstructed coronal field configurations can effectively demonstrate the multi-wavelength observations for flare/CME events**
- **Future missions, Solar-B, SDO, will provide better data for understand the nature of the Sun**
- **Efforts to combine both large-scale and small-scale field are needed and fast computing techniques should be developed.**

Thanks!